Biologically interpretable deep learning to predict response to immunotherapy in advanced melanoma using mutations and copy number variations

Liuchao Zhang
Harbin Medical University
Lei Cao
Harbin Medical University
Shuang Li
Harbin Medical University
Liuying Wang
Harbin Medical University
Yongzhen Song
Harbin Medical University
Yue Huang
Harbin Medical University
Zhenyi Xu
Harbin Medical University
Jia He
Harbin Medical University
Meng Wang
Harbin Medical University
Kang Li (likang@ems.hrbmu.edu.cn)
Harbin Medical University

Research Article

Keywords: Immunotherapy, Advanced melanoma, Deep learning model, Predictive biomarker, KEGG pathways, Multi-omics

Posted Date: July 1st, 2022

DOI: https://doi.org/10.21203/rs.3.rs-1784695/v1

Abstract

Only 30–40% of advanced melanoma patients respond effectively to immunotherapy in clinical practice, so it's necessary to accurately identify the response of melanoma patients to immune therapy pre-clinically. Here we developed the KP-NET, a deep learning model whose structure is sparse by the KEGG pathways, which can accurately predict melanoma patients' response to immunotherapy using information at the pathway level that is enriched from gene mutations and copy number variations data prior to immune therapy. The KP-NET demonstrated the best performance on predictive melanoma response to anti-CTLA-4 and anti-PD-1 treatment with corresponding AUROC values of 0.889 and 0.867, and selected some relevant biomarkers, genes such as PLCB2, FGFR4, RHEB and CCNB2, pathways such as Inflammatory mediator regulation of TRP channels, Notch signaling pathway, mTOR signaling pathway and TNF signaling pathway, etc. In conclusion, deep learning model guided by biological information enables accurate prediction of the response of melanoma patients to immunotherapy and relevant biomarkers before clinical treatment, which may be helpful in melanoma precision medicine.

Introduction

Immune checkpoint inhibitors (ICIs) include monoclonal antibodies targeting the immune inhibitory proteins programmed cell death protein 1 (PD-1) and cytotoxic T lymphocyte-associated antigen 4 (CTLA-4)[1]. While ICIs have resulted in durable clinical response in melanoma, only 30–40% of patients generate objective clinical response[2, 3]. Therefore, biomarkers and models that accurately predict ICIs treatment response in melanoma patients are necessary. Using these biomarkers and models, we can screen patients for the best response to immunotherapy, maximizing patients' benefits and minimizing the costs.

A number of biomarkers associated with immunotherapy response have been identified, such as tumor mutational burden (TMB) and neoantigen load[4–6] and alternative survival and proliferation pathway[7]. Nevertheless, these biomarkers have some drawbacks, for example, non-standardized cut-off value, relatively high cost-effectiveness, unsatisfactory predictive power restrict their clinical application, and their predictive contributions to response or resistance of ICIs remain largely uncharacterized[8]. Due to the limitations above, some genomic studies suggest that mutations and copy number variations (CNVs) affecting particular genes and signaling pathways have additional ability to predict response of ICIs[9–13]. Therefore, we need a predictive model using patients' mutation and CNVs profiles that not only exhibits good predictive performance, but also can screen some important biomarkers.

Although several predictive models have been proposed in previous studies, many of them face challenges of trade-off between model interpretability and accuracy. For example, linear models such as logistic regression usually has good interpretability but poor predictive performance, whereas deep learning model such as fully connected neural network (FNN) often has less interpretability but higher predictive performance, and it is computationally expensive and tends to overfit[14–16]. In order to overcome the limitations above, Ma et al.[17] developed Dcell based on visible neural network to model

the effect of gene interaction on cell growth in yeast, and Kuenzi et al.[18] proposed DrugCell, an interpretable deep learning model to predict drug response and synergy. Hao et al.[19] built PASNet, a pathway-associated sparse deep neural network to predict prognosis of Glioblastoma multiforme. The sparsification of PASNet not only reduced the number of model parameters to avoid overfitting, but also took advantage of biological knowledge. Elmarakeby et al.[20] developed a sparse network (P-NET) based on pathways from Reactome and further calculated importance score for each gene and pathway using DeepLIFT[14] method.

Here, we built a KEGG pathway neural network (KP-NET) to predict advanced melanoma patients' response to ICIs treatment. The most distinct innovative aspects of KP-NET proposed are as follows: (1) Based on our limited knowledge, our study is the first to predict immune response using somatic mutations and CNVs data which obtained from pre-immunotherapy tissue. (2) We use the KEGG pathways which is simpler to sparse neural network, significantly reducing the number of model parameters and avoiding overfitting while utilizing biological information. (3) To further avoid overfitting, we add batch normalization layer and dropout layer to the KP-NET. (4) The KP-NET can accurately predict the response of melanoma patients to anti-PD-1 and anti-CTLA-4 treatment and identify relevant biomarkers to provide some insights for clinical immunotherapy.

Materials And Methods

Clinical Cohorts

We collated clinical information, mutations and copy number data of melanoma patients therapied with ICIs from previous published articles. A total of 122 advanced melanoma patients treated with anti-CTLA-4 inhibitor and whose tissue was obtained before immunotherapy were selected from Dana-Farber Cancer Institute[21], we named it as anti-CTLA-4 Data Set, and the exclusion criteria is shown in Fig. 1. In addition, a total of 144 metastatic melanoma patients treated with anti-PD-1 inhibitor between January 2013 and June 2016[22] were also included, excluding one patient whose tissue was taken after anti-PD-1 therapy and 9 patients who had received more than 2 remaining treatments prior to anti-PD-1 inhibitors, we selected 134 patients as anti-PD-1 Data Set.

Melanoma patients' best response to anti-CTLA-4 or anti-PD-1 inhibitor was assessed according to RECIST criteria v1.1, patients achieving complete response (CR), partial response (PR) or stable disease (SD) / mixed response (MR) were grouped as responders, whereas patients showing progressive disease (PD) were referred to as non-responders.

For somatic mutations data, only non-silent mutated genes were included in our following analysis. In order to avoid the bias of low mutation ratio genes on KP-NET model's prediction performance, we further excluded genes whose mutated rate was less than 5%.

For copy number data in anti-CTLA-4 Data Set, CNVs were considered amplified or deleted if the $|\log_2(\text{copy ratio})|$ exceeded 0.5, genes were annotated with R packages 'CNTools', and genes in which variation rate less than 10% were excluded. The copy number data in anti-PD-1 Data Set was preprocessed as in Liu et al. [22], it was inspected visually and manually for focal amplifications and deletions, and genes were annotated with Oncotator[23]. Furthermore, only genes whose variation rate exceeded 5% were retained in anti-PD-1 Data Set.

Kp-net Model

The KP-NET is a biologically informed sparse neural network, which could accurately predict response of ICIs therapy in patients with melanoma using their genomic profiles. Inspired by the KEGG Pathway Maps[24], every node in KP-NET represents a biological entity, such as genes and pathways, each edge encodes a known relationship between the corresponding entities (Fig. 2). The architecture of KP-NET is composed of five layers, the nodes in input layer represent patients' genomic features, including mutation, copy number amplification and copy number deletion. The second layer represents genes of interest, each node in this layer is exactly connected to the input layer. The remaining three layers represent pathways from KEGG, and higher layers represent more abstract and complex biological processes. Combining KEGG pathway information with deep learning, KP-NET not only significantly reduces the number of parameters, but also demonstrates the state of different biological entities.

Sparse connections between inputs and genes or genes and pathways are encoded using a mask matrix M, which multiplies the weights matrix W to zero-out all the connections that not exist. The output of each sparse layer is calculated as

$$\hat{y} = (M \odot W)^T x + b$$

,

where M is mask matrix, W is weights matrix, x is input matrix, b is bias vector, and $\odot$ represents Hadamard product. Each sparse layer in KP-NET is paired with batch normalization layer, ReLU activation function and dropout layer. The final output layer is paired with a softmax activation function to transform outcomes of KP-NET into class probabilities.

DeepLIFT is a backpropagation-based attribution method, which can calculate a sample-level importance score for each node in our KP-NET. Given a sample s and its input features $x^s = (x_1^s, \ldots, x_i^s, \ldots, x_n^s)$, where n also is the number of nodes in the KP-NET's input layer. we can gain the predicted value $\hat{y}^s$ by feeding its features into the KP-NET, that is,

$$\hat{y}^s = f\left(x^s\right)$$

where f represents the KP-NET. If we set the reference of x^s as $x_0^s = (x_{1_0}^s, ..., x_{i_0}^s, ..., x_{n_0}^s)$, we also can obtain the reference of $\hat{y}^s$ by

$$\hat{y}_0^s = f\left(x_0^s\right)$$

Then, an importance score C_i^s of the i-th feature in sample s is calculated based on the difference in target activation $\Delta\hat{y}^s = \hat{y}^s - \hat{y}_0^s$, and $\Delta\hat{y}^s$ equals sum of all features' importance scores. That is,

$$\Delta\hat{y}^s = \sum_{i=1}^{n} C_i^s$$

To obtain the final sample-level importance C_i, we aggregated the score C_i^s over all the n_s samples

$$C_i = \left|\sum_{s=1}^{n_s} C_i^s\right|$$

In this way, we can calculate the importance score of each node in the KP-NET. Usually, nodes with more connected edges are more likely to have larger importance scores. So, we use d_i that is the number of edges connected with node i to adjust its score C_i,

$$AdjC_i = \begin{cases} \frac{C_i}{d_i}, & d_i > \mu + 2\sigma \\ C_i, & otherwise \end{cases}$$

where μ and σ are the mean and standard deviation of d_i, respectively.

Kp-net Training And Evaluation

In order to check out the utility of KP-NET, we train it to predict response states (responder/non-responder) of melanoma patients to anti-CTLA-4 or anti-PD-1 ICIs. For anti-CTLA-4 Data Set and anti-PD-1 Data Set, we randomly split each of them into a discovery set (80%) and a target set (20%). When we perform hyperparameter optimization for KP-NET, the discovery set is further divided into a training set (60% of discovery set), a validation set (20% of discovery set) and a test set (20% of discovery set). We use the validation set for early stopping while training KP-NET, but concatenate it into training set for other methods which do not need a validation set. The test set is used to select the optimal set of hyperparameters. When we perform 5-fold cross-validation, the discovery set is only partitioned into a training set (80% of discovery set) and a validation set (20% of discovery set) for each cross-validation fold, and the validation set in each fold is not overlapped.

When training the KP-NET model, Adam optimizer with an initial learning rate of 0.01 and weight decay of 1×10^{-5} is used. The learning rate is decayed by λ_{γ} after every n_{step} epochs for a smooth convergence. The epoch number of early stopping is 50 and the size of mini-batches is set to 8. Besides, we further perform a grid search to optimize (1) learning rate decay ratio ($\lambda_{\gamma} \in [0.95, 0.9]$), (2) learning rate decay step size ($n_{step} \in [20, 30]$), (3) dropout probability ($p_{drop} \in [0.1, 0.2, 0.3]$).

Meanwhile, we also perform hyperparameter optimization for baseline methods. For random forest (RF), we optimize the trees' number ($N_{RF} \in [100, 200, 500, 1000]$). For the support vector machine (SVM), we optimize the regularization strength parameter ($C \in 10^{k}, \forall k \in [-3, -2, -1, 0, 1]$). For the AdaBoost, the number of decision tree ($N_{AB} \in [50, 100, 200, 500]$) is optimized.

The statistical analysis of clinical characteristics between the discovery set and the target set is performed using R 4.1.0. The deep learning models are implemented using PyTorch modules (version 1.7.1). The baseline methods are performed using scikit-learn modules (version 0.24.2). The source code is available at https://github.com/0219zhang/KP-NET.

Result

Response to anti-CTLA-4 treatment

The clinical characteristics including age, gender and histology between anti-CTLA-4 treatment discovery set ($n = 97$) and target set ($n = 25$) were not significantly different. There were 60 (61.86%) patients with PD after anti-CTLA-4 therapy in discovery set, which was not significantly different with 16 (64%) PD patients in target set in terms of clinical characteristics. The details were shown in Table 1.

For predicting response to anti-CTLA-4 treatment of patients in the target set, compared with baseline methods, such as RF, SVM, logistic regression, decision tree and AdaBoost, the KP-NET showed best performance (area under the receiver operating characteristic curve (AUROC) = 0.889, area under the precision-recall curve (AUPR) = 0.933, accuracy = 0.76, F1-score = 0.842) (Fig. 3a and 3b), which indicates that the KP-NET can extract better biological features by integrating KEGG pathways while having the nonlinear fitting ability of deep learning model .

In order to evaluate whether sparse model had different performance compared with dense fully connected model. We trained a dense model named Dense1 which had the same number of nodes and layers as KP-NET, and another dense model named Dense2 with the same number of parameters as KP-NET, both of them achieved inferior performance (Fig. 3a and 3b), indicating that sparsification of deep learning model using biological knowledge can indeed improve its predictive performance. Meanwhile, the trained KP-NET model exactly classified 100% of the responders and 72.73% of the non-responders with anti-CTLA-4 ICIs, demonstrating the potentials of the KP-NET for clinical applications (Fig. 3c). Moreover, the AUROC, AUPR, accuracy and F1-score of five-fold cross-validation showed that the KP-NET

model had a stable predictive performance, with a mean AUROC of 0.856, where its standard deviation was just 0.041 (Fig. 3d).

In order to understand the interactions between input features, genes and pathways that contributed to predictive performance and display the information flow from the inputs to outcomes, we visualized the trained KP-NET model with fully interpretable layers. Due to the large number of genes and pathways, we only showed the top 10 nodes with the highest importance scores in each layer of the KP-NET (Fig. 4).

Clearly, mutation data provided more information than copy number variants when we predicted response to anti-CTLA-4 inhibitor in melanoma patients. Among the 10 most important genes selected by KP-NET, we could see that PLCB2, ADCY1 and MAPK8 genes were enriched in Inflammatory mediator regulation of TRP channels, the most important pathway selected. There were also other important genes including FGFR4, COL1A2, GANI1 and so on. Meanwhile, in the most important pathways screened by the KP-NET, there was a well-known tumor-related pathway, Notch signaling pathway. We noticed that genes with higher scores tend to be enriched in pathways with higher scores, indicating the reasonableness of the integration of the KP-NET and DeepLIFT.

Response to anti-PD-1 treatment

In this dataset, the gender and histology between the discovery set and the target set also were not significant difference. There were 49 (45.79%) patients with PD after anti-PD-1 therapy in the discovery set and 12 (44.44%) PD patients in the target set (P>0.05). The clinical characteristics are detailed in Table 2.

Compared to baseline methods, the KP-NET model still showed best performance when predicted response to anti-PD-1 therapy, that AUROC = 0.867, AUPR = 0.834, accuracy = 0.76, F1-score = 0.842 (Fig. 5a and 5b), and exactly classified 85.71% of the melanoma responders with anti-PD-1 ICIs and 76.92% of the non-responders (Fig. 5c). The result of 5-fold cross-validation further demonstrated the stability of KP-NET model (Fig. 5d). The results demonstrated the promising applicability of the KP-NET in predicting response to immunotherapy, either for anti-CTLA-4 or anti PD-1 ICIs, in melanoma patients.

The information flowing and entities importance for predicting anti-PD-1 response were interpretable visualized in Fig. 6. The CNVs data was more informative than mutations when employed to predict anti-PD-1 response, which was different from anti-CTLA-4 ICIs. Among the 10 most important genes, the first gene RHEB was connected with AMPK signaling pathway and mTOR signaling pathway, and the second gene CREB3L1 was enriched in AMPK signaling pathway and TNF signaling pathway. All these pathways above were well-known for their association with tumor. Besides, some of the other pathways, such as NF-kappa B signaling pathway and TGF-beta signaling pathway, were with high importance scores. We can also find a strong connectivity between genes and pathways with high importance scores, which is consistent with the results of the KP-NET in predicting response of anti-CTLA-4 ICIs.

Discussion

The KP-NET is a deep neural network with structured sparsification using KEGG pathways information which has a relatively simple structure. The sparsification process guided by KEGG pathways can significantly improve the prediction capability of the KP-NET by reducing the number of trainable parameters in the KP-NET while using biological information to enrich gene information to the pathway level. Meanwhile, we add batch normalization layer and drop out layer to the KP-NET to improve its robustness. Due to the strong feature extraction capability of the KP-NET, we can accurately predict the response to immunotherapy in melanoma patients using their pre-treatment multi-omics data. In the two case studies of predicting response to anti-CTLA-4 and anti-PD-1 inhibitors in melanoma, the KP-NET demonstrated the best prediction performance, significantly outperforming baseline methods such as RF and SVM, as well as FNNs with same number of nodes, layers and parameters as the KP-NET, demonstrating the feasibility and accuracy of integrating KEGG pathways information. Moreover, the KP-NET screens some biomarkers of response to immunotherapy in melanoma by combining with DeepLIFT algorithm, which may be helpful in clinical practice.

Among the genes and pathways screened by the KP-NET in the mission of predicting response to anti-CTLA-4 therapy in melanoma, Inflammatory mediator regulation of TRP channels with the highest importance score includes genes PLCB2, ADCY1 and MAPK8. Studies have found that all these genes could contribute to the transition of inflammation and immune response and further affect response to anti-CTLA-4 ICIs[25], and these three genes were also identified as potential prognostic biomarkers for melanoma[26–29]. The other genes including FGFR4, GNAI1, CD36 and FLT1 could alter the tumor microenvironment and further impact ICIs' clinical efficacy, combination their inhibitors and ICIs might be better for melanoma[30–33]. Khunger et al.[34] found that COL1A2 was associated with cancer development and progression, and patients with melanoma were more likely to be benefit from anti-CTLA-4 inhibitors when COL1A2 was highly expressed. Moreover, for the Notch signaling pathway, Cho et al.[35]found that it could affect activation of cytotoxic T cells, inflammatory immune microenvironment, inflammatory expression profile and immunogenicity, and Li et al.[36] reported that patients with non-small cell lung cancer (NSCLC) treated by ICIs could own longer survival time if they had high-mutated Notch signaling. These results suggest that the genes and pathways screened by the KP-NET combined with DeepLIFT are credible to predict response to immunotherapy in melanoma patients.

Similarly, the candidate genes selected by the KP-NET are biologically significant in predicting the response of melanoma to anti-PD-1 inhibitor. For example, genes RHEB and CREB3L1 enriched in mTOR signaling pathway and AMPK signaling pathway not only contributed to predict response to anti-PD-1 inhibitor, but also could regulate PD-1 expression, increase expansion of effector T cells, reduce the emergence of immune escape and display antitumor effect in murine tumor models[37–39]. Among the remaining genes, Chen et al.[40] found that CCNB2 could serve as a marker to predict response to anti-PD-1 therapy in NSCLC patients, suggesting that CCNB2 might also be a predictor of response to anti-PD-1 treatment in melanoma. For another important gene TNFRSF11A, also named RANK, a clinical trial combining its monoclonal antibody and Immune checkpoint inhibitors for the treatment of melanoma were already underway[41]. The other genes such as IFNA13, ACTG1 and PPP2R1B all involved in immune-regulatory activities, playing distinctive roles in melanoma cells' focal adhesion and motility[42–

45]. Therefore, the proposed KP-NET may have a great potential on discovering important biomarkers in immunotherapy of advanced melanoma.

There also are some limitations in our study. The sample size of both datasets used in our research is not particularly large, more samples would be used in our future study to verify the predictive ability of the KP-NET. In addition, the biological relationships we used were obtained from KEGG pathway database, we will further explore the influence of other pathway databases, such as Gene Ontology, to guide network's architecture.

In conclusion, our KP-NET model could not only accurately classify response versus non-response for immunotherapy to melanoma patients, but also reveal related biological mechanism.

Declarations

Funding

This work was supported by National Nature Science Foundation of China (project number 81973149 and 81773551).

Competing Interests

The authors declare that they have no conflicts of interest with the publication of the manuscript.

Author Contributions

Liuchao Zhang wrote the code to achieve different tasks; Liuchao Zhang and Kang Li designed the experiments; Liuchao Zhang and Lei Cao wrote the manuscript with assistance and feedback of all the co-authors; Shuang Li, Liuying Wang and Yongzhen Song collected and interpreted the data. Yue Huang, Zhenyi Xu, Jia He and Meng Wang prepared figures. All authors read and approved the final manuscript.

Data availability

The Raw anti-CTLA-4 Data Set is publicly available available at dbGaP under accession number phs001565.v1.p1. The Raw anti-PD-1 Data Set are available in dbGaP (accession number phs000452.v3.p1). The data used and/or analyzed during the current study are available from the corresponding author on reasonable request.

Ethics approval

Not applicable.

Consent to participate

Not applicable.

Consent to publish

Not applicable.

References

1. Topalian SL, Taube JM, Anders RA, Pardoll DM (2016) Mechanism-driven biomarkers to guide immune checkpoint blockade in cancer therapy. Nature reviews. Cancer. 16: 275-87. doi: 10.1038/nrc.2016.36
2. Topalian SL, Hodi FS, Brahmer JR et al. (2012) Safety, activity, and immune correlates of anti–PD-1 antibody in cancer. New England Journal of Medicine. 366: 2443-54.
3. Hamid O, Robert C, Daud A et al. (2013) Safety and tumor responses with lambrolizumab (anti–PD-1) in melanoma. New England Journal of Medicine. 369: 134-44.
4. Rizvi NA, Hellmann MD, Snyder A et al. (2015) Cancer immunology. Mutational landscape determines sensitivity to PD-1 blockade in non-small cell lung cancer. Science (New York, N.Y.). 348: 124-8. doi: 10.1126/science.aaa1348
5. Snyder A, Makarov V, Merghoub T et al. (2014) Genetic basis for clinical response to CTLA-4 blockade in melanoma. The New England journal of medicine. 371: 2189-99. doi: 10.1056/NEJMoa1406498
6. Cristescu R, Mogg R, Ayers M et al. (2018) Pan-tumor genomic biomarkers for PD-1 checkpoint blockade-based immunotherapy. Science (New York, N.Y.). 362. doi: 10.1126/science.aar3593
7. George S, Miao D, Demetri GD et al. (2017) Loss of PTEN Is Associated with Resistance to Anti-PD-1 Checkpoint Blockade Therapy in Metastatic Uterine Leiomyosarcoma. Immunity. 46: 197-204. doi: 10.1016/j.immuni.2017.02.001
8. Bai X, Wu DH, Ma SC et al. (2020) Development and validation of a genomic mutation signature to predict response to PD-1 inhibitors in non-squamous NSCLC: a multicohort study. Journal for immunotherapy of cancer. 8. doi: 10.1136/jitc-2019-000381
9. Riaz N, Havel JJ, Kendall SM, Makarov V, Walsh LA, Desrichard A, Weinhold N, Chan TA (2016) Recurrent SERPINB3 and SERPINB4 mutations in patients who respond to anti-CTLA4 immunotherapy. Nature genetics. 48: 1327-9. doi: 10.1038/ng.3677
10. Johnson DB, Lovly CM, Flavin M et al. (2015) Impact of NRAS mutations for patients with advanced melanoma treated with immune therapies. Cancer immunology research. 3: 288-95. doi: 10.1158/2326-6066.cir-14-0207
11. Gao J, Shi LZ, Zhao H et al. (2016) Loss of IFN-γ Pathway Genes in Tumor Cells as a Mechanism of Resistance to Anti-CTLA-4 Therapy. Cell. 167: 397-404.e9. doi: 10.1016/j.cell.2016.08.069
12. Kato S, Goodman A, Walavalkar V, Barkauskas DA, Sharabi A, Kurzrock R (2017) Hyperprogressors after Immunotherapy: Analysis of Genomic Alterations Associated with Accelerated Growth Rate. Clinical cancer research : an official journal of the American Association for Cancer Research. 23: 4242-50. doi: 10.1158/1078-0432.ccr-16-3133

13. Miao D, Margolis CA, Gao W et al. (2018) Genomic correlates of response to immune checkpoint therapies in clear cell renal cell carcinoma. Science (New York, N.Y.). 359: 801-6. doi: 10.1126/science.aan5951
14. Shrikumar A, Greenside P, Kundaje A (2017) Learning important features through propagating activation differences. Proceedings of the 34th International Conference on Machine Learning - Volume 70. JMLR.org, Sydney, NSW, Australia. pp. 3145–53
15. Murdoch WJ, Singh C, Kumbier K, Abbasi-Asl R, Yu B (2019) Definitions, methods, and applications in interpretable machine learning. Proceedings of the National Academy of Sciences of the United States of America. 116: 22071-80. doi: 10.1073/pnas.1900654116
16. Xu Q, Zhang M, Gu Z, Pan G (2019) Overfitting remedy by sparsifying regularization on fully-connected layers of CNNs. Neurocomputing. 328: 69-74. doi: https://doi.org/10.1016/j.neucom.2018.03.080
17. Ma J, Yu MK, Fong S, Ono K, Ideker T (2018) Using deep learning to model the hierarchical structure and function of a cell. Nature Methods. 15.
18. Kuenzi BM, Park J, Fong SH, Sanchez KS, Lee J, Kreisberg JF, Ma J, Ideker T (2020) Predicting Drug Response and Synergy Using a Deep Learning Model of Human Cancer Cells. Cancer Cell. 38: 672-84.e6.
19. Hao J, Kim Y, Kim T-K, Kang M (2018) PASNet: pathway-associated sparse deep neural network for prognosis prediction from high-throughput data. BMC Bioinformatics. 19: 510. doi: 10.1186/s12859-018-2500-z
20. Elmarakeby HA, Hwang J, Arafeh R et al. (2021) Biologically informed deep neural network for prostate cancer discovery. Nature. 598: 348-52. doi: 10.1038/s41586-021-03922-4
21. Miao D, Margolis CA, Vokes NI et al. (2018) Genomic correlates of response to immune checkpoint blockade in microsatellite-stable solid tumors. Nature genetics. 50: 1271-81. doi: 10.1038/s41588-018-0200-2
22. Liu D, Schilling B, Liu D et al. (2019) Integrative molecular and clinical modeling of clinical outcomes to PD1 blockade in patients with metastatic melanoma. Nature medicine. 25: 1916-27. doi: 10.1038/s41591-019-0654-5
23. Ramos AH, Lichtenstein L, Gupta M, Lawrence MS, Pugh TJ, Saksena G, Meyerson M, Getz G (2015) Oncotator: cancer variant annotation tool. Human mutation. 36: E2423-9. doi: 10.1002/humu.22771
24. Kanehisa M, Goto S (2000) KEGG: kyoto encyclopedia of genes and genomes. Nucleic acids research. 28: 27-30. doi: 10.1093/nar/28.1.27
25. Parenti A, De Logu F, Geppetti P, Benemei S (2016) What is the evidence for the role of TRP channels in inflammatory and immune cells? British journal of pharmacology. 173: 953-69. doi: 10.1111/bph.13392
26. Zhang H, Xie T, Shui Y, Qi Y (2020) Knockdown of PLCB2 expression reduces melanoma cell viability and promotes melanoma cell apoptosis by altering Ras/Raf/MAPK signals. Molecular medicine reports. 21: 420-8. doi: 10.3892/mmr.2019.10798

27. Chen J, Wu F, Shi Y, Yang D, Xu M, Lai Y, Liu Y (2019) Identification of key candidate genes involved in melanoma metastasis. Molecular medicine reports. 20: 903-14. doi: 10.3892/mmr.2019.10314
28. Luo H, Ma C (2021) A Novel Ferroptosis-Associated Gene Signature to Predict Prognosis in Patients with Uveal Melanoma. Diagnostics (Basel, Switzerland). 11. doi: 10.3390/diagnostics11020219
29. Noman MZ, Berchem G, Janji B (2018) Targeting autophagy blocks melanoma growth by bringing natural killer cells to the tumor battlefield. Autophagy. 14: 730-2. doi: 10.1080/15548627.2018.1427398
30. Katoh M (2016) FGFR inhibitors: Effects on cancer cells, tumor microenvironment and whole-body homeostasis (Review). International journal of molecular medicine. 38: 3-15. doi: 10.3892/ijmm.2016.2620
31. Wu Y, Jia H, Zhou H, Liu X, Sun J, Zhou X, Zhao H (2022) Immune and stromal related genes in colon cancer: Analysis of tumour microenvironment based on the cancer genome atlas (TCGA) and gene expression omnibus (GEO) databases. Scandinavian journal of immunology. 95: e13119. doi: 10.1111/sji.13119
32. Ma X, Xiao L, Liu L et al. (2021) CD36-mediated ferroptosis dampens intratumoral CD8(+) T cell effector function and impairs their antitumor ability. Cell metabolism. 33: 1001-12.e5. doi: 10.1016/j.cmet.2021.02.015
33. Lacal PM, Atzori MG, Ruffini F et al. (2020) Targeting the vascular endothelial growth factor receptor-1 by the monoclonal antibody D16F7 to increase the activity of immune checkpoint inhibitors against cutaneous melanoma. Pharmacological research. 159: 104957. doi: 10.1016/j.phrs.2020.104957
34. Khunger A, Piazza E, Warren S et al. (2021) CTLA-4 blockade and interferon-α induce proinflammatory transcriptional changes in the tumor immune landscape that correlate with pathologic response in melanoma. PloS one. 16: e0245287. doi: 10.1371/journal.pone.0245287
35. Cho OH, Shin HM, Miele L, Golde TE, Fauq A, Minter LM, Osborne BA (2009) Notch regulates cytolytic effector function in CD8+ T cells. Journal of immunology (Baltimore, Md. : 1950). 182: 3380-9. doi: 10.4049/jimmunol.0802598
36. Li X, Wang Y, Li X, Feng G, Hu S, Bai Y (2021) The Impact of NOTCH Pathway Alteration on Tumor Microenvironment and Clinical Survival of Immune Checkpoint Inhibitors in NSCLC. Frontiers in Immunology. 12. doi: 10.3389/fimmu.2021.638763
37. Veliça P, Zech M, Henson S et al. (2015) Genetic Regulation of Fate Decisions in Therapeutic T Cells to Enhance Tumor Protection and Memory Formation. Cancer research. 75: 2641-52. doi: 10.1158/0008-5472.can-14-3283
38. Ye J (2013) Roles of regulated intramembrane proteolysis in virus infection and antiviral immunity. Biochimica et biophysica acta. 1828: 2926-32. doi: 10.1016/j.bbamem.2013.05.005
39. Pokhrel RH, Acharya S, Ahn JH et al. (2021) AMPK promotes antitumor immunity by downregulating PD-1 in regulatory T cells via the HMGCR/p38 signaling pathway. Molecular cancer. 20: 133. doi: 10.1186/s12943-021-01420-9

40. Chen S, Liu Z, Li M et al. (2020) Potential Prognostic Predictors and Molecular Targets for Skin Melanoma Screened by Weighted Gene Co-expression Network Analysis. Current gene therapy. 20: 5-14. doi: 10.2174/1566523220666200516170832
41. Ahern E, Cubitt A, Ballard E et al. (2019) Pharmacodynamics of Pre-Operative PD1 checkpoint blockade and receptor activator of NFkB ligand (RANKL) inhibition in non-small cell lung cancer (NSCLC): study protocol for a multicentre, open-label, phase 1B/2, translational trial (POPCORN). Trials. 20: 753. doi: 10.1186/s13063-019-3951-x
42. Bianchi M, Alisi A, Fabrizi M, Vallone C, Ravà L, Giannico R, Vernocchi P, Signore F, Manco M (2019) Maternal Intake of n-3 Polyunsaturated Fatty Acids During Pregnancy Is Associated With Differential Methylation Profiles in Cord Blood White Cells. Frontiers in genetics. 10: 1050. doi: 10.3389/fgene.2019.01050
43. Malek N, Mrówczyńska E, Michrowska A, Mazurkiewicz E, Pavlyk I, Mazur AJ (2020) Knockout of ACTB and ACTG1 with CRISPR/Cas9(D10A) Technique Shows that Non-Muscle β and γ Actin Are Not Equal in Relation to Human Melanoma Cells' Motility and Focal Adhesion Formation. International journal of molecular sciences. 21. doi: 10.3390/ijms21082746
44. Richter C, Mayhew D, Rennhack JP, So J, Stover EH, Hwang JH, Szczesna-Cordary D (2020) Genomic Amplification and Functional Dependency of the Gamma Actin Gene ACTG1 in Uterine Cancer. International journal of molecular sciences. 21. doi: 10.3390/ijms21228690
45. Jiang SL, Wang ZB, Zhu T, Jiang T, Fei JF, Liu C, Luo C, Cheng Y, Liu ZQ (2021) The Downregulation of eIF3a Contributes to Vemurafenib Resistance in Melanoma by Activating ERK via PPP2R1B. Frontiers in pharmacology. 12: 720619. doi: 10.3389/fphar.2021.720619

Tables

Table 1. Clinical characteristics of anti-CTLA-4 discovery set and target set

	Total (n=122)	Discovery (n=97)	Target (n=25)	z/χ^2	*P*
Age *M(Q1, Q3)*	62(45.5,73)	65(47,73)	54(42.75,71.5)	1.37	0.1707
Gender *n*(%)				0.27	0.6054
female	34(27.87)	26(26.8)	8(32)		
male	88(72.13)	71(73.2)	17(68)		
Histology *n(%)*				0.01	0.9069
cutaneous/mucosal	101(82.79)	81(83.51)	20(80)		
other	21(17.21)	16(16.49)	5(20)		
RECIST *n(%)*				-	0.7891
CR	8(6.56)	7(7.22)	1(4)		
PR	20(16.39)	17(17.53)	3(12)		
SD	18(14.75)	13(13.4)	5(20)		
PD	76(62.3)	60(61.86)	16(64)		

The number of melanoma patients with given characteristic is shown, the number in parentheses representing the corresponding percentage. - represents Fisher's exact test

Table 2. Clinical characteristics of anti-PD-1 discovery set and target set

	Total (n=134)	Discovery (n=107)	Target (n=27)	χ^2	*P*
Gender *n*(%)				0.83	0.362
female	55(41.04)	46(42.99)	9(33.33)		
male	79(58.96)	61(57.01)	18(66.67)		
Histology *n(%)*				0.09	0.7638
cutaneous/mucosal	107(79.85)	86(80.37)	21(77.78)		
other	27(20.15)	21(19.63)	6(22.22)		
RECIST *n(%)*				-	0.5087
CR	16(11.94)	14(13.08)	2(7.41)		
PR	35(26.12)	25(23.36)	10(37.04)		
SD	22(16.42)	19(17.76)	3(11.11)		
PD	61(45.52)	49(45.79)	12(44.44)		

The number of melanoma patients with given characteristic is shown, the number in parentheses representing the corresponding percentage. - represents Fisher's exact test

Figures

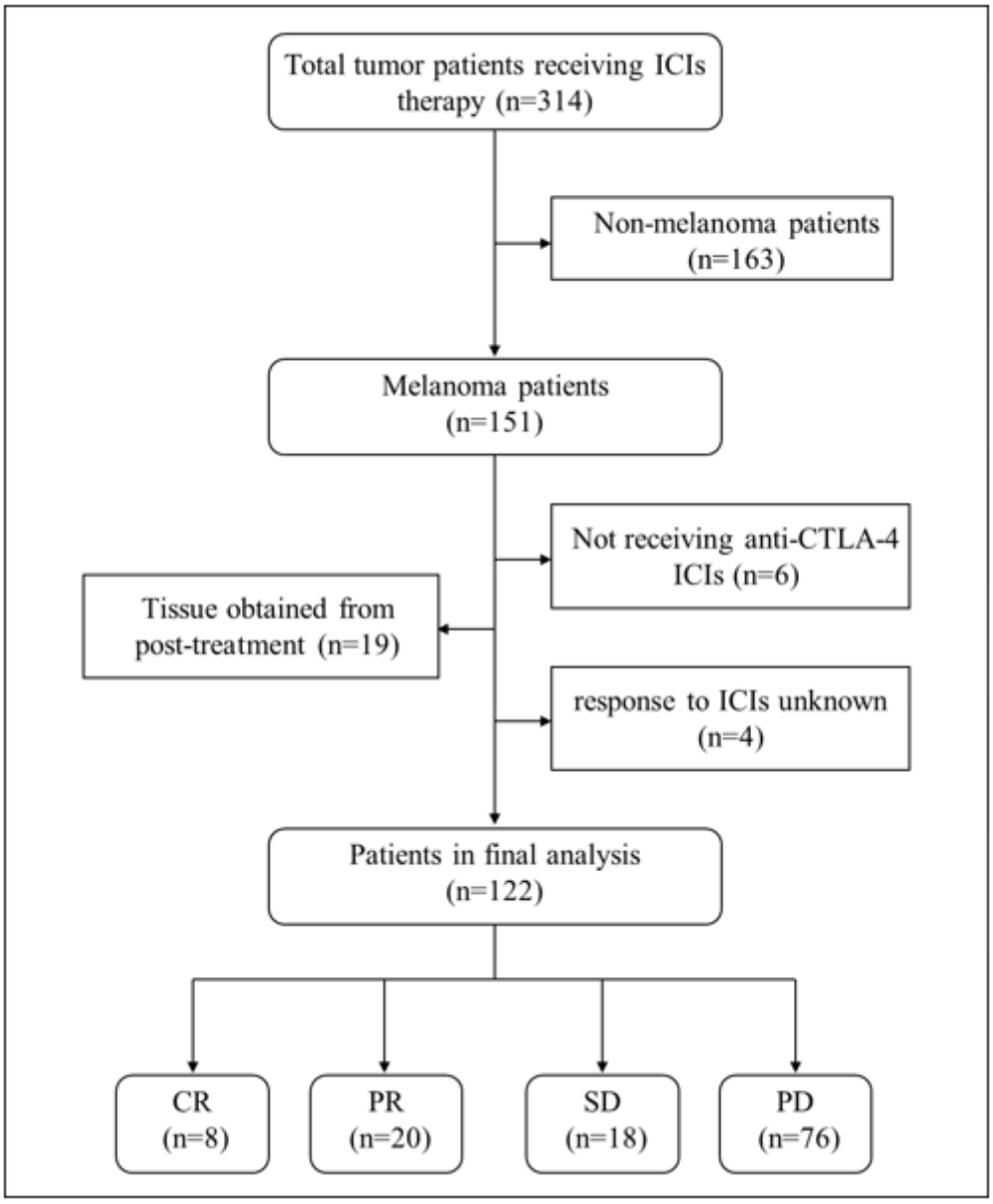

Figure 1

The process of screening samples for the anti-CTLA-4 Data Set

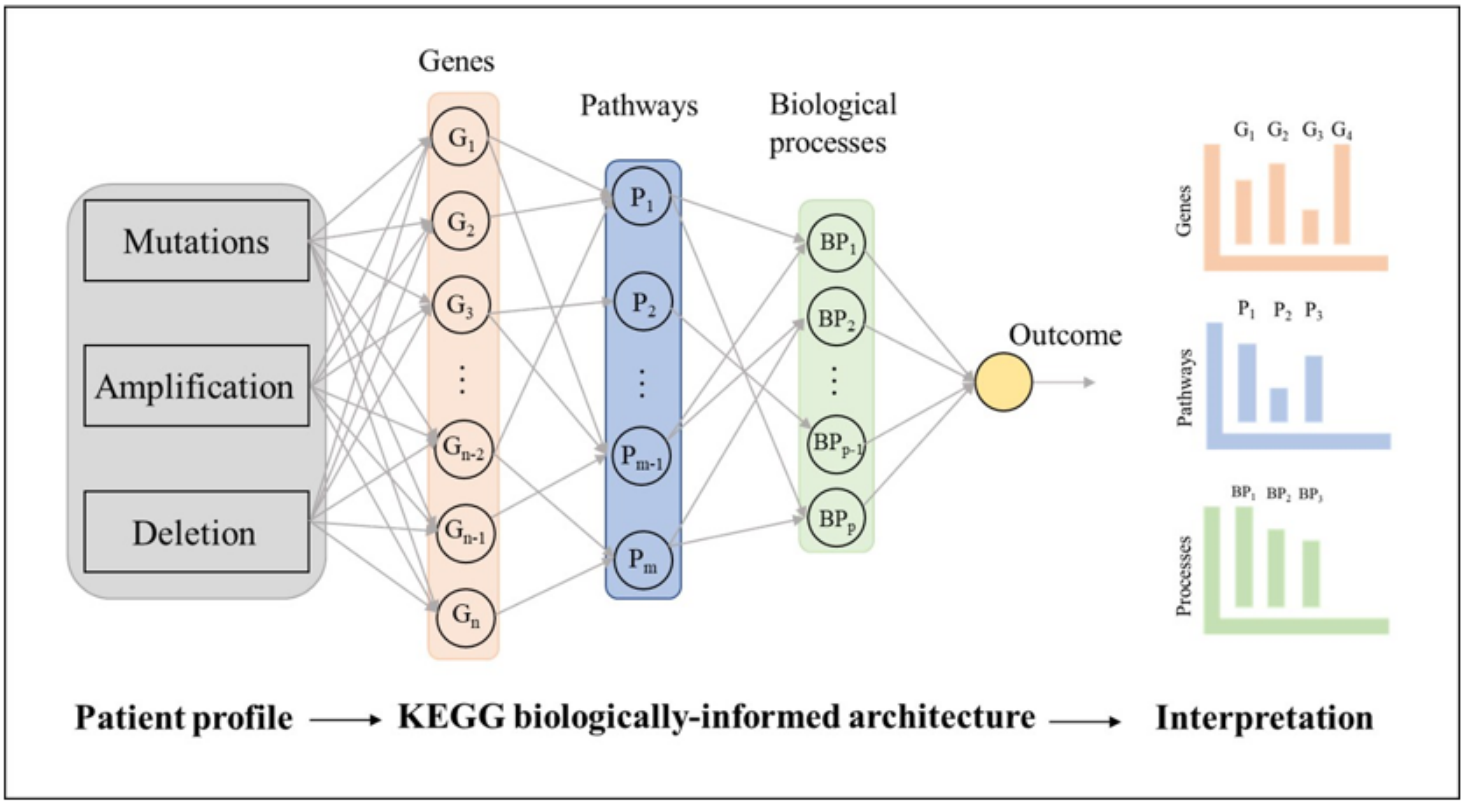

Figure 2

Schematic diagram of KP-NET. The nodes in different layers encodes different biological entities, such as features from patient genomic profile, genes and pathways. The edges between adjacent layers are biologically customized to show the information flow from inputs to outcome

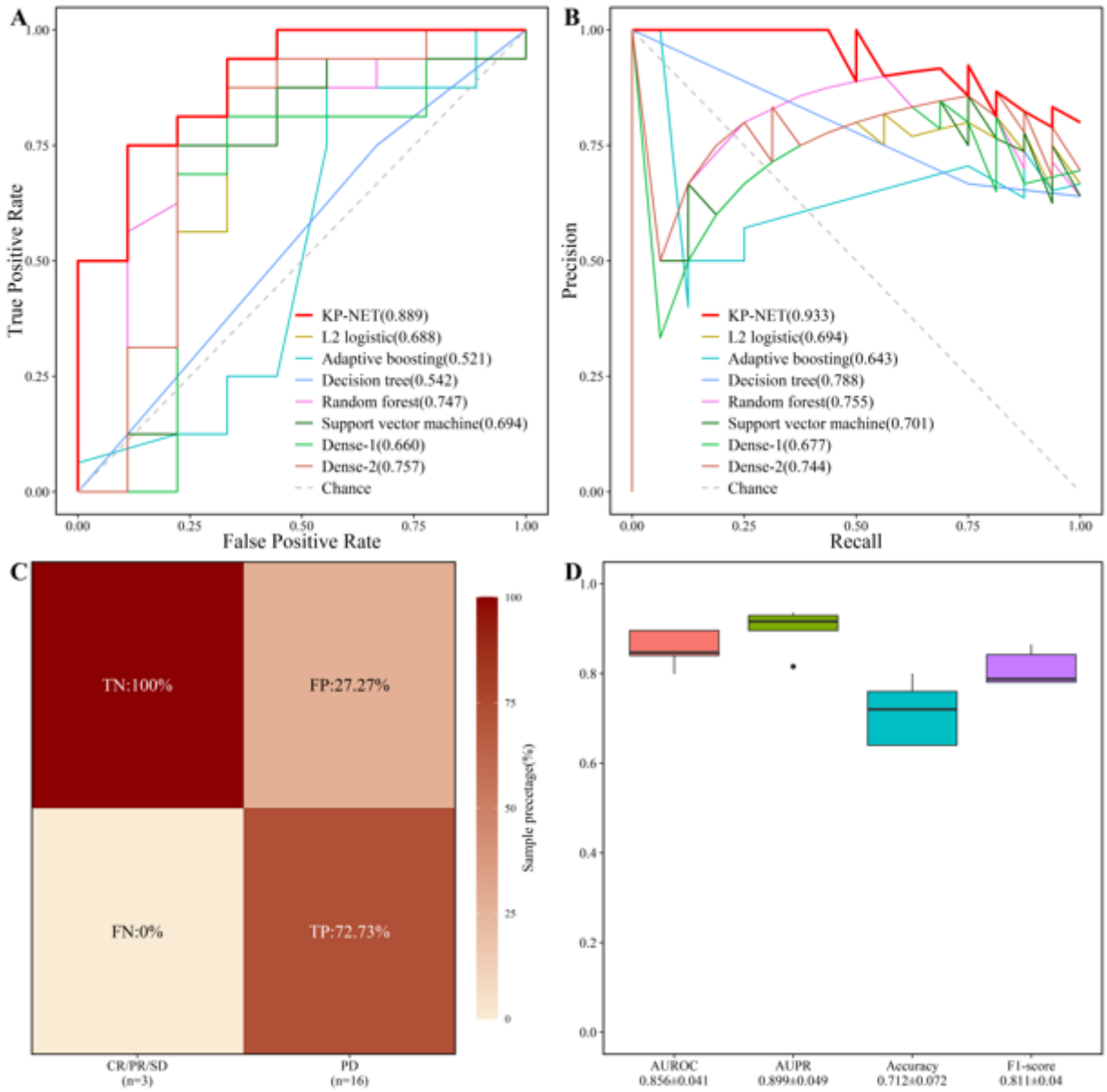

Figure 3

Prediction performance of KP-NET on anti-CTLA-4 Data Set. a ROC curve of eight methods. b PR curve of eight methods. c confusion matrix using KP-NET model to classify the target set. d Metrics of 5-fold cross-validation of KP-NET, which also are represented by mean±standard deviation

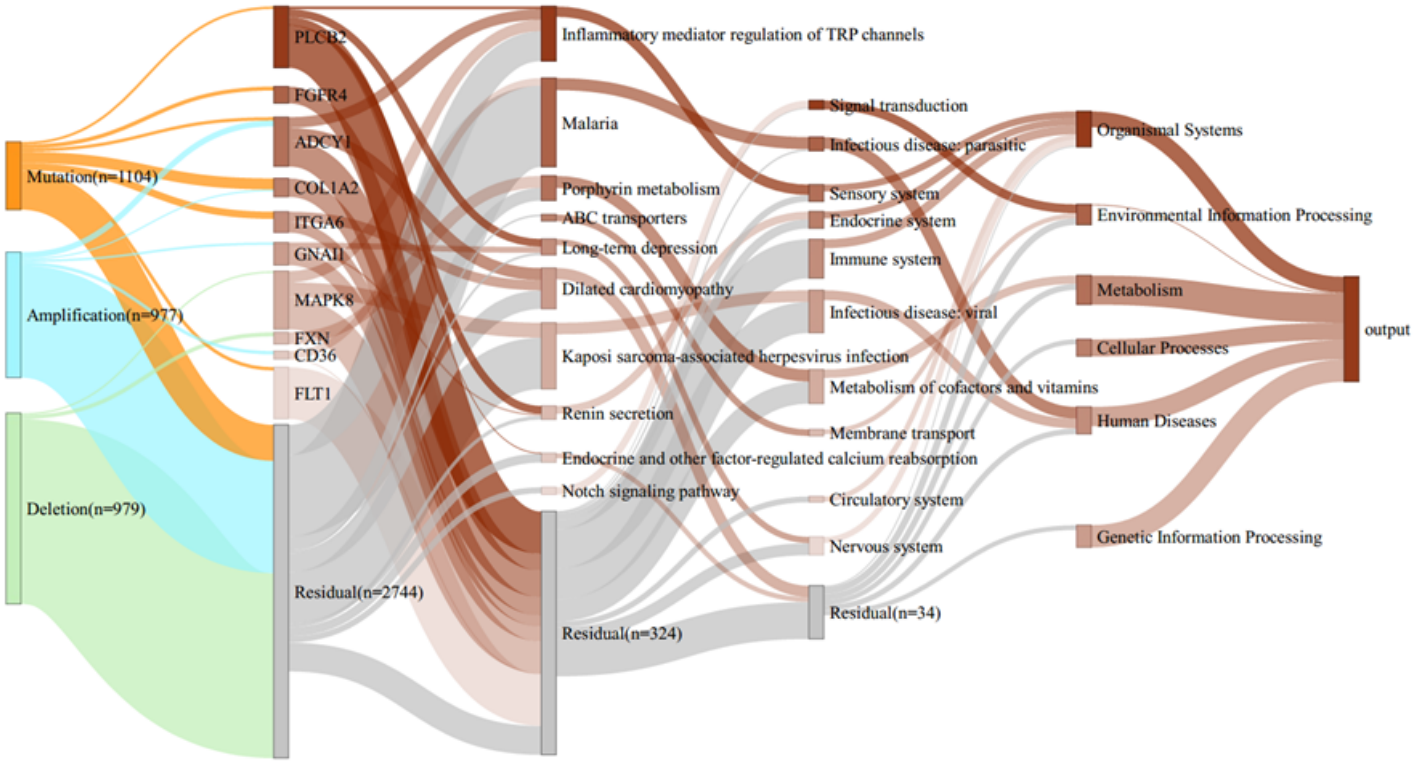

Figure 4

Sankey diagram interpreting KP-NET on anti-CTLA-4 Data Set. Visualization of the whole KP-NET shows the relative importance of nodes in each layer. Darker color's nodes are more important, while grey nodes which named 'Residual' show the residual importance of the others nodes in each layer. The value in parentheses indicate the total number of nodes included in the category, for example, there are 2744 genes categorized as 'Residual'. TRP, transient receptor potential

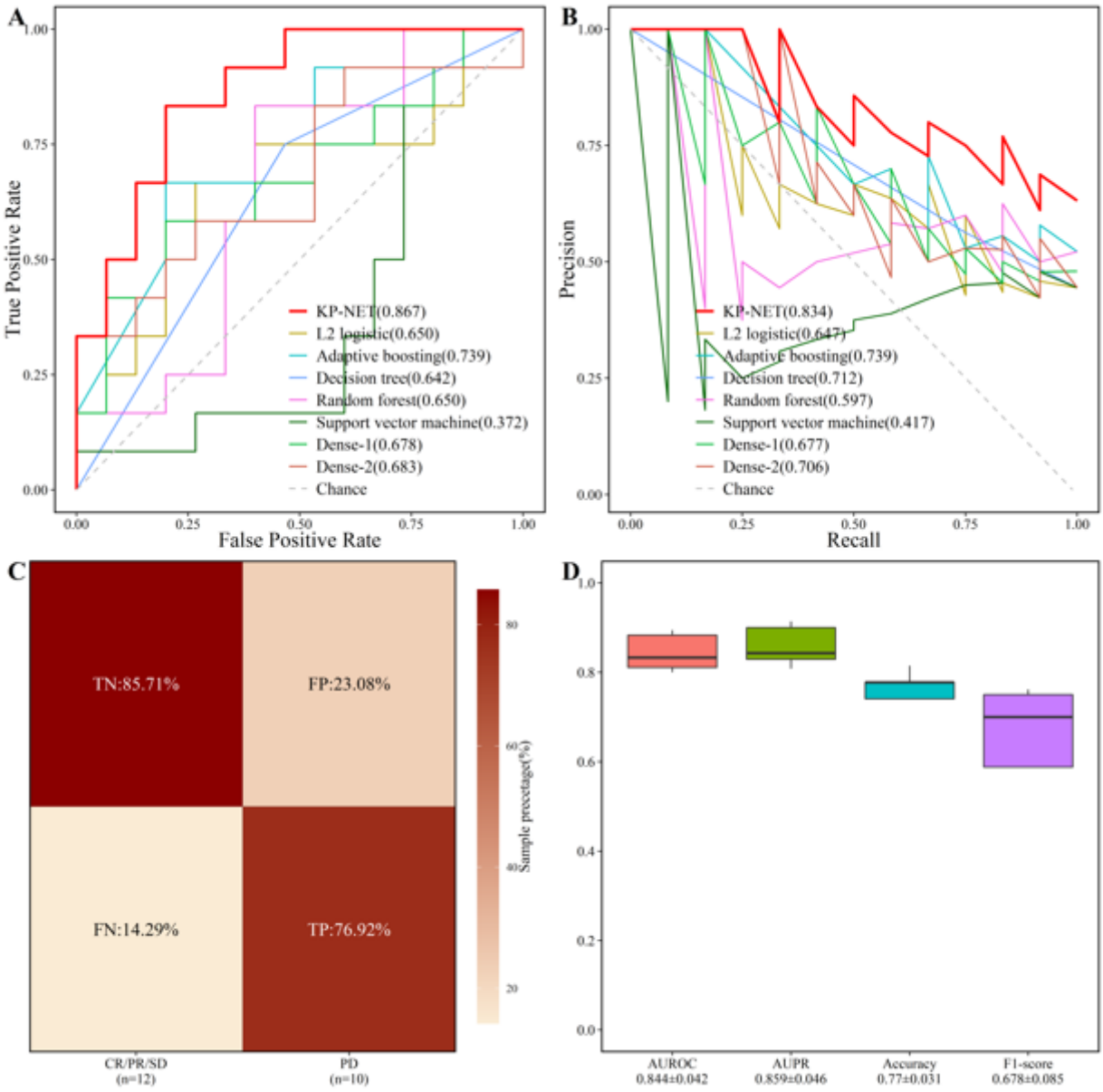

Figure 5

Prediction performance of KP-NET on anti-PD-1 Data Set. a ROC curve of eight methods. b PR curve of eight methods. c Confusion matrix using KP-NET model to classify the target set. d Metrics of 5-fold cross-validation of KP-NET, which also are represented by mean±standard deviation

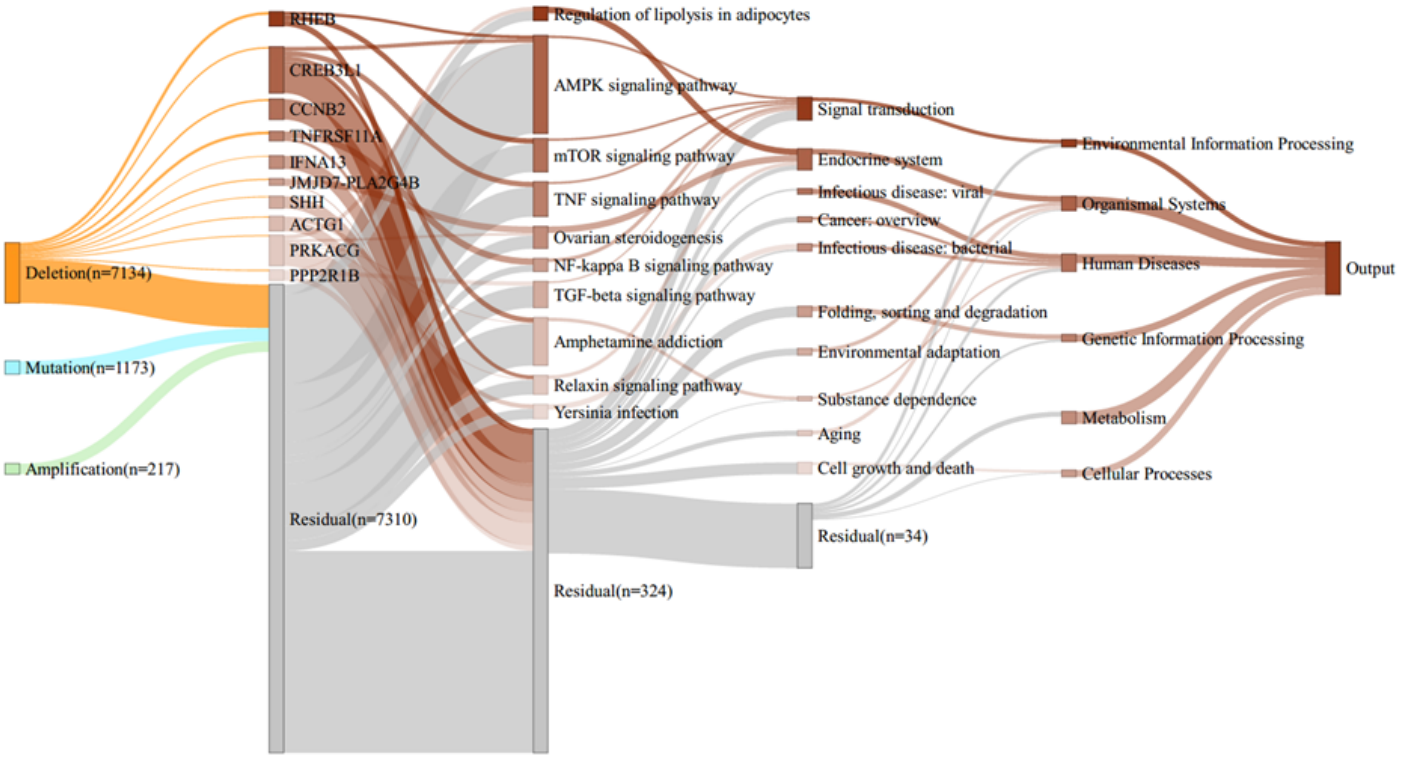

Figure 6

Sankey diagram interpreting KP-NET on anti-PD-1 Data Set. Visualization of the whole KP-NET shows the relative importance of nodes in each layer. Darker color's nodes are more important, while grey nodes which named 'Residual' show the residual importance of the others nodes in each layer. The value in parentheses indicate the total number of nodes included in the category